

**CLEEN**

Cluster for Energy and Environment

**Research report no. D4.4-3  
Helsinki 2015**

C. Bajamundi, M. Aho, K. Korpijärvi  
VTT Technical Research Centre of Finland Ltd.

**The fate of cobalt, copper, and antimony during  
combustion of waste wood  
(A thermodynamic equilibrium study)**



---

**arvi**

Material Value Chains

---



arvi

Material Value Chains

The fate of Co, Cu, and Sb during  
combustion of waste wood.  
C. Bajamundi, M. Aho, K. Korpijärvi

2(26)

**CLEEN OY**  
ETELÄRANTA 10  
00130 HELSINKI  
FINLAND  
[www.cleen.fi](http://www.cleen.fi)

ISBN 978-952-5947-82-3  
ISSN XXXX-XXXX



**arvi**

Material Value Chains

The fate of Co, Cu, and Sb during  
combustion of waste wood.  
C. Bajamundi, M. Aho, K. Korpijärvi

3(26)

**Cleen Oy**  
Research report no D4.4-3

Cyril Bajamundi, Martti Aho, Kirsi Korpijärvi  
VTT Technical Research Centre of Finland Ltd.

# **The fate of cobalt, copper, and antimony during combustion of waste wood (A thermodynamic equilibrium study)**



**Name of the report: The fate of cobalt, copper, and antimony during combustion of waste wood (A thermodynamic equilibrium study)**

**Key words: cobalt; copper; antimony; waste wood; combustion; thermodynamic equilibrium**

## Summary

Fly ashes from the combustion of fuels such as waste wood, solid recovered fuels and other fuels derived from waste may contain high concentration of metals that can be of economic value when recovered. On the other hand, their presence can result in classification of fly ash as problematic waste with high cleaning costs increasing significantly energy production costs in the particular power plant. To enable recovery of these metals, it is important to understand how they behave during the combustion process - from fuel feeding up to fly ash and flue gas release.

In this report, the behaviour of cobalt, copper, and antimony during the combustion of waste wood was analysed. The model showed that these elements have different fates inside a bubbling fluidized bed boiler. Co is found mostly in the molten phase, Cu can be found in all phases (gas, solid, melt), while Sb is mostly in the gas phase.

Variation in the concentration of Cl and S in the waste wood fuel had little effect in the phase partitioning of these elements. Increasing the Cl concentration from 0.05 wt.% d.s. to 0.36 wt.% d.s. did not change the phase partitioning of Co and Sb, while there is a slight enhancement of gas phase partitioning of Cu. Increasing the S concentration from 0.04 wt.% d.s. to 0.09 wt.% d.s. also did not change the phase partitioning of Co and Sb, while there is an enhancement of molten phase partitioning of Cu.

Simulation of elemental sulphur addition (at  $S_{\text{total}}/Cl_{\text{fuel}} = 3.0$ ) revealed that the phase partition of Co and Sb is, in general, similar to the base case. That is Co is found mostly in the molten phase and Sb is mostly in the gas phase. Cu however showed enhanced phase partitioning in the molten phase relative to the base case.

Using these results a concept that could potentially enrich Sb in-situ boiler is proposed.

Helsinki, September 2015



## Contents

<b>1</b>	<b>Description and objectives .....</b>	<b>1-6</b>
<b>2</b>	<b>Fuel and Methods .....</b>	<b>2-8</b>
<b>3</b>	<b>Results.....</b>	<b>3-12</b>
<b>3.1</b>	<b>Base case: Phase partitioning of Co, Cu, and Sb .....</b>	<b>3-12</b>
3.1.1	Cobalt.....	3-12
3.1.2	Copper.....	3-13
3.1.3	Antimony .....	3-14
<b>3.2</b>	<b>Sensitivity Analysis: Effect of varying Cl concentration .....</b>	<b>3-15</b>
3.2.1	Cobalt.....	3-15
3.2.2	Copper.....	3-16
3.2.3	Antimony .....	3-17
3.2.4	Summary of importance of varying Cl concentration .....	3-17
<b>3.3</b>	<b>Sensitivity Analysis: Effect of varying S concentration .....</b>	<b>3-18</b>
3.3.1	Cobalt.....	3-18
3.3.2	Copper.....	3-19
3.3.3	Antimony .....	3-20
3.3.4	Summary of importance of varying S concentration .....	3-20
<b>4</b>	<b>Effect of Additive .....</b>	<b>4-21</b>
<b>5</b>	<b>Discussion.....</b>	<b>23</b>
<b>6</b>	<b>Conclusion and recommendation .....</b>	<b>25</b>
<b>7</b>	<b>References .....</b>	<b>26</b>

## 1 Description and objectives

In a typical boiler facility, the elements in the fuel can end up as part of the bottom ash, fly ash, or flue gas, see Figure 1. Concentration of each element in the exit stream is dependent on the behaviour of the particular element in the boiler system. For example, non-volatile elements such as silicon and aluminium may be enriched in the bottom ash or the coarse fraction of the fly ash. Volatile elements of the fuel such as Na and K salts etc. vaporize in the lower part of the boiler to condense later (like in the 2nd pass or after it) and end up being part of the finer fraction of the fly ash. C, H, O, N and S form major components of the flue gas.

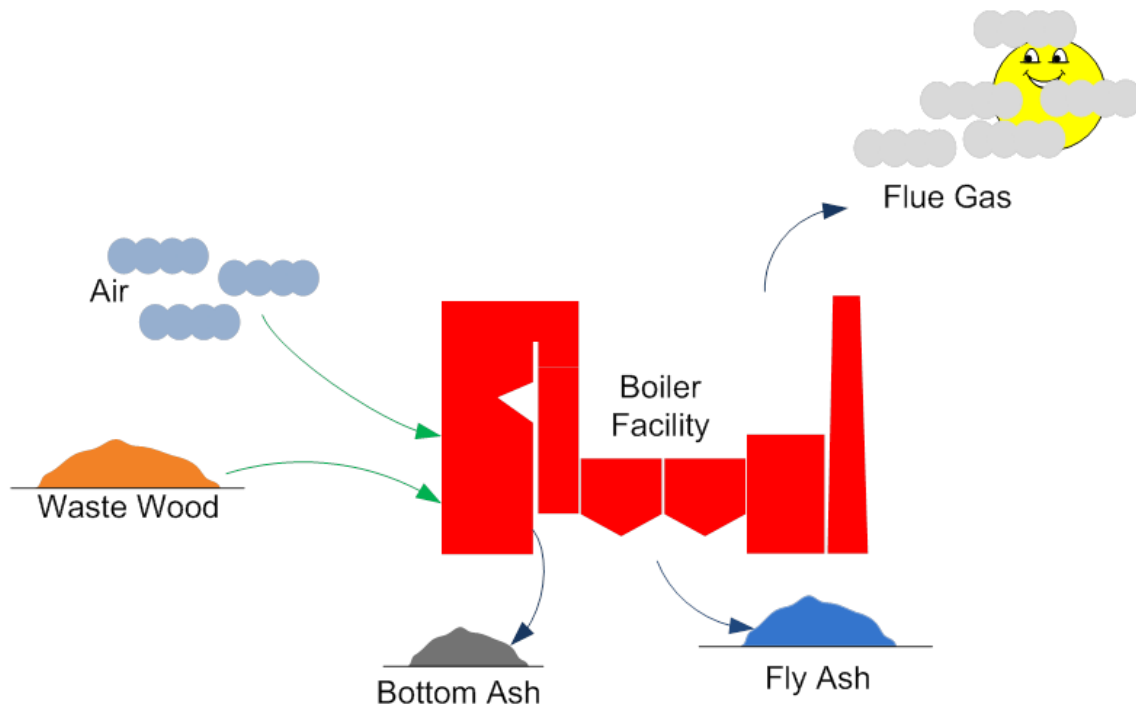


Figure 1. Simplified mass streams in a typical boiler facility.

For trace elements found in the fuel, Clarke and Sloss have classified these elements according to their relative volatility [1], see Figure 2. Group 1 elements are non-volatile and are enriched in the bottom ash. Group 2 elements are concentrated in the particulates and may be present in the fine particle fractions of fly ash. They undergo volatilisation upon combustion and later condense in the colder zones of the boiler. Group 3 elements are very volatile and may remain permanently in the gas phase during combustion.

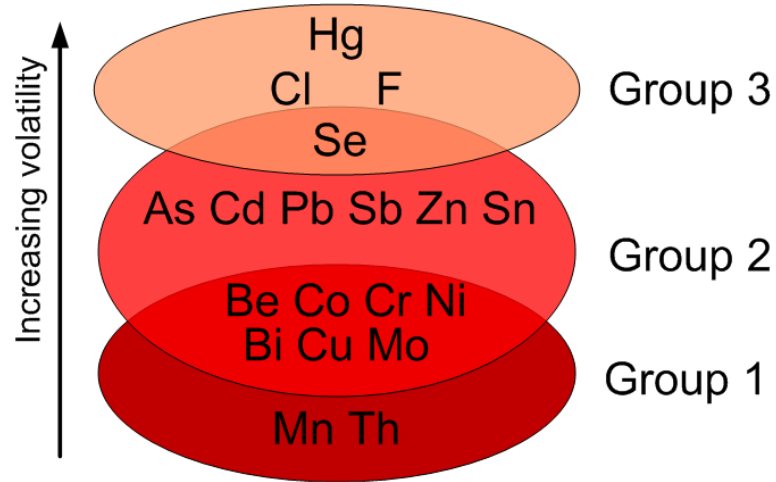


Figure 2. Classification of trace elements by their volatility during combustion [1].

Understanding the behaviour of critical elements is essential in for (a) boiler operation – to assess the risk of corrosion, and ash melting or slagging (b) emission – to meet limits set by applicable directives, (c) recovery of important elements in the ash (d) improved quality of major fly ash stream to reduce ash treatment costs.

The main objective of this study is to use thermodynamic equilibrium modelling to explore the fate of cobalt, copper, and antimony during the combustion of waste wood. The goal is to understand where Co, Cu, and Sb end up during combustion of the fuel and find ways to drive these elements to a certain ash fraction.



## 2 Fuel and Methods

The main fuel studied is waste wood. Table 1 shows a typical composition of waste wood. The concentration of C, H, S, O, and N as well as ash forming elements (Al, Ti, Na, Mg, K, Fe and P) did not vary significantly. Heavy metals such as Cu, Pb, Ba, and Zn have the highest variation in concentration.

**Table 1. Typical of composition of waste wood**

FUEL : Waste Wood			Value			
			mean	median	min	max
Proximate analysis	H <sub>2</sub> O	wt-%	26.75	25.30	21.70	37.30
	volatiles	wt-% (d.s.)	78.17	78.05	76.90	79.50
	fixed carbon	wt-% (d.s.)	18.67	18.55	17.60	19.70
	ash (815 °C)	wt-% (d.s.)	3.16	3.00	2.10	4.40
	ash (550°C)	wt-% (d.s.)	3.37	3.35	2.20	4.80
Ultimate analysis (dry solids)	C	wt-% (d.s.)	48.81	48.80	48.50	49.20
	H	wt-% (d.s.)	6.15	6.20	5.90	6.40
	S	wt-% (d.s.)	0.07	0.07	0.04	0.09
	O	wt-% (d.s.)	39.77	39.68	38.77	40.52
	N	wt-% (d.s.)	1.86	1.91	1.25	2.52
	Cl	wt-% (d.s.)	0.17	0.13	0.05	0.36
	F	wt-% (d.s.)	0.00	0.00	0.00	0.00
	Br	wt-% (d.s.)	0.00	0.00	0.00	0.00
Element concentrations in the dry substance	Al	g/kg	1.09	1.10	0.65	1.40
	Si	g/kg	5.83	6.30	2.90	7.40
	Ti	g/kg	1.45	1.45	1.20	1.80
	Na	g/kg	0.84	0.84	0.71	1.10
	Mg	g/kg	0.50	0.49	0.38	0.65
	K	g/kg	0.85	0.87	0.66	0.98
	Ca	g/kg	3.98	3.90	2.60	5.20
	Fe	g/kg	0.81	0.82	0.47	1.10
	P	g/kg	0.13	0.14	0.07	0.21
Heavy metals concentrations in the dry substance	Sb	mg/kg	6.46	5.10	1.20	15.00
	As	mg/kg	14.55	10.55	7.70	46.00
	Cd	mg/kg	0.77	0.69	0.29	1.50
	Cr	mg/kg	29.30	27.00	17.00	45.00
	Co	mg/kg	1.86	1.40	0.98	6.30
	Cu	mg/kg	83.10	30.00	20.00	580.00
	Pb	mg/kg	148.50	155.00	32.00	310.00
	Mn	mg/kg	83.90	84.50	75.00	93.00
	Hg	mg/kg	0.07	0.06	0.00	0.27
	Ni	mg/kg	6.66	6.55	2.50	11.00
	Tl	mg/kg	0.00	0.00	0.00	0.00
	Sn	mg/kg	3.31	2.50	0.68	9.40
	V	mg/kg	1.99	1.75	1.00	5.00
	Ba	mg/kg	207.00	210.00	130.00	290.00
	Mo	mg/kg	0.53	0.60	0.00	0.96
	Se	mg/kg	0.00	0.00	0.00	0.00
	Zn	mg/kg	255.40	245.00	94.00	460.00

Figure 3 shows the mean concentration of the fuel components and their variation. To help visualize the difference/similarity of the properties of waste wood and typical compositions of reference fuels (straw and coniferous wood) are also included.

The concentration of the major components of the waste wood and the reference fuel are nearly similar. For the elements S to P, the concentration in the waste wood is somewhere between the coniferous wood (low values) and straw (high values). The concentration of



trace elements such as Cu, Pb, Ba and Zn are highest in the waste wood relative to the reference fuels.

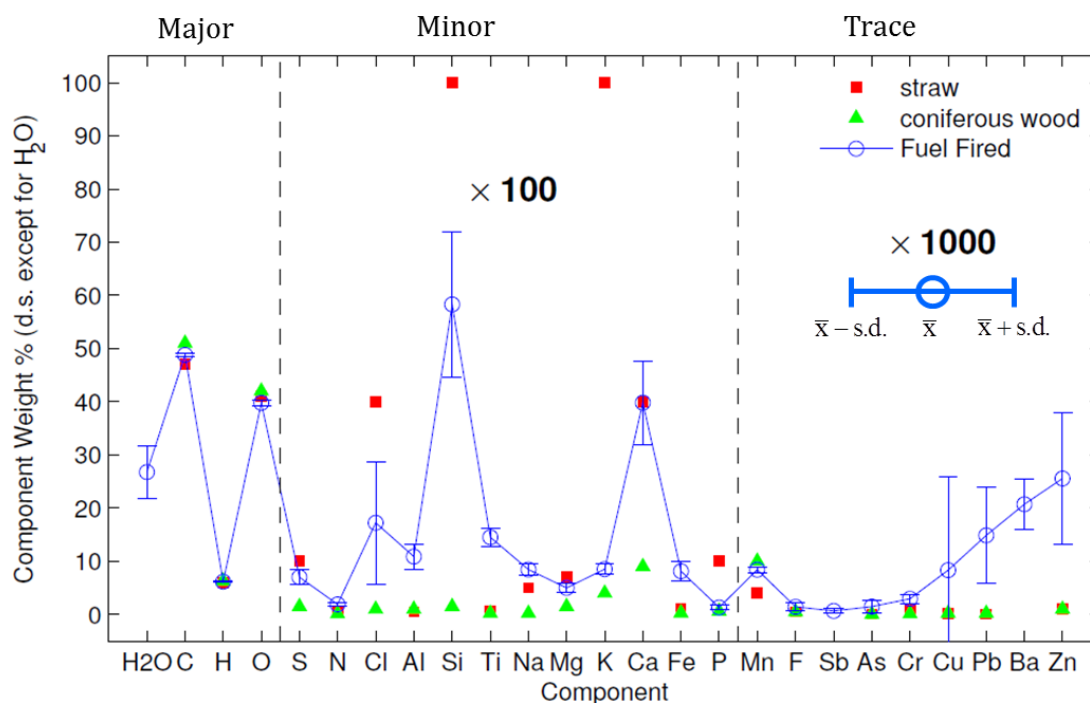


Figure 3. Mean concentration of components of waste wood, straw, coniferous wood.  $\bar{x}$  = mean, s.d. = standard deviation.

Thermodynamic equilibrium modelling is the tool used to examine the behaviour of waste wood during combustion. The model is based on the minimization of the total Gibbs energy of a given system and is implemented in FactSage 6.4. The structure of the model is shown in Figure 4.

Thermodynamic equilibrium calculations have been used to analyse systems such as combustion [2–4], gasification [5], cement kiln chemistry [6] and several others. The flexibility of the computation approach and the rapid growth in computing power enabled systematic calculation of multi-phase multi-component equilibrium systems. Equilibrium calculations give accurate results in high temperature applications because the assumptions of the calculations are met. One assumption is rapid reaction which essentially renders the reaction to approach equilibrium. This assumption is true for high temperature systems.

The quality of the database used in the simulation also greatly determines the output of equilibrium calculation. Talonen used five commercial databases (HSC, FACT,SGTE, IVTANTHERMO and JANAF) to study the behaviour of 12 heavy metals regulated in the WID and noted significant variation in this thermodynamic databases [7]. The algorithm for performing Gibbs minimization also affects the outcome of the result. For example, HSC handles only pure substances while FactSage can handle both pure and solution databases.



In addition the applicability of thermodynamic equilibrium modelling can be limited by local temperature gradients, physical processes such as adsorption and capillary condensation, non-ideal mixing behaviour between different ash forming elements and the mode of occurrence of components in the fuel which dictates its release or retention rate [8,9]. However, clever and carefully designed methodologies can produce valuable information about overall stabilities and speciation trends [10].

The calculations were performed using global approach at 1 atm and air-to-fuel ratio ( $\lambda$ ) range of 0.4 – 1.6 corresponding to the reducing and oxidizing conditions in the combustion system. The temperature range simulated is 500°C to 1200°C.

The database used in the calculation contains gas and pure solid species as well as solution species (oxides and salts). The database used are from FactPS, FTOxid and FTSalt, these are thermodynamic databases that come part of FactSage 6.4. FTOxid and FTSalt represent the molten or liquid phases.

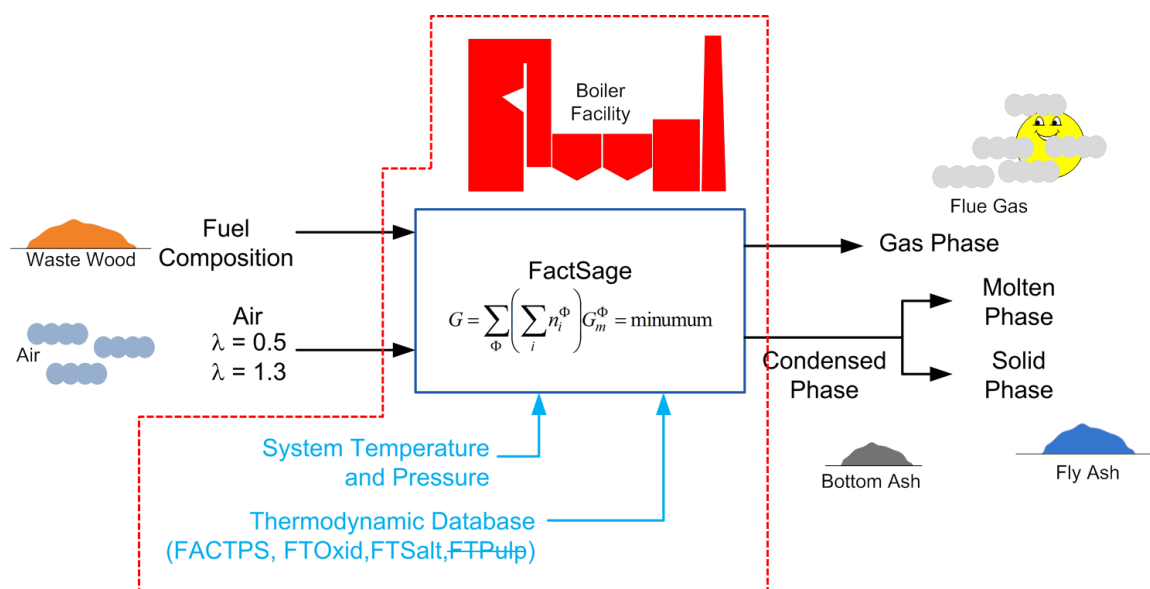


Figure 4. Features of the thermodynamic equilibrium modelling.

To determine in what phase (gas, condensed) a certain element will end up, we introduce the phase partitioning ratio,  $\phi$ . Phase partitioning is defined as the amount of the element ending up in a particular phase relative to the amount of element in the fuel fed.

$$\phi_{i,j} = \frac{\text{mole of element } i \text{ in phase } j}{\text{mole of element } i \text{ in fuel}} \quad 1$$

If  $j = \text{gas}$ ,  $\phi_{i,gas}$  is the measure of how volatile ( $\phi_{i,gas} \rightarrow 1$ ) or non-volatile ( $\phi_{i,gas} \rightarrow 0$ ) an element is during combustion.



Phase partitioning is calculated as a function of  $T$  and  $\lambda$ . Visualizing this data requires a 3D plot; however for ease of presentation (without loss of information) the plot presented here is the top view projection of the 3D surface (Figure 5).

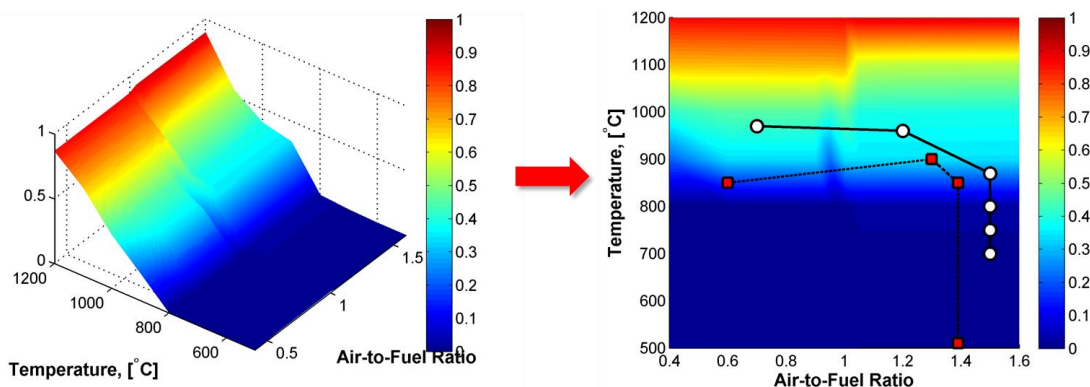


Figure 5. Sample representation of the result.

To put results into perspective, two samples bubbling fluidized bed boiler profiles are superimposed to aid in interpreting the results, see Figure 6. The splash zone is the region just above the bed where the fuel and primary air first meet. The secondary and tertiary air zones are near the location of the secondary air and tertiary air injection, respectively.

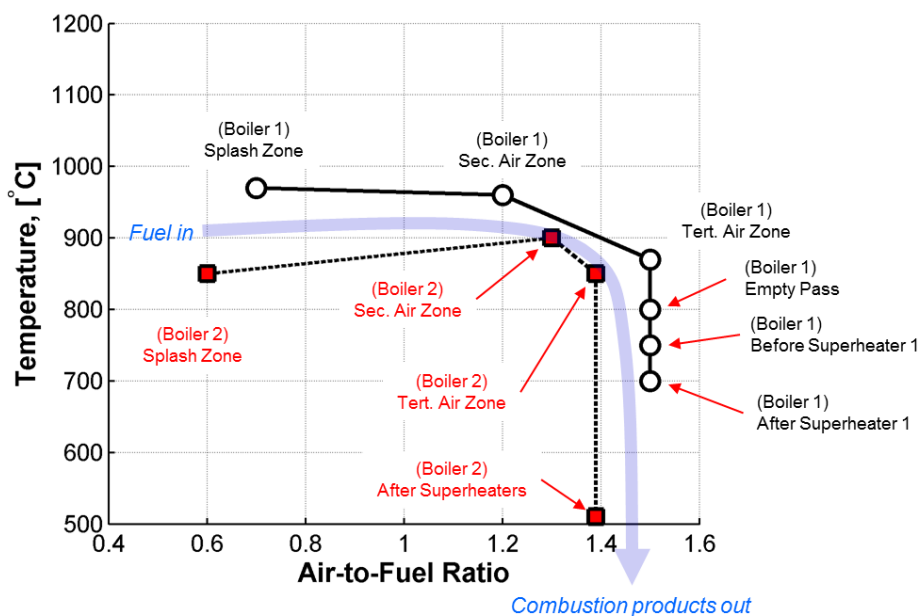


Figure 6. Gas temperature profiles for typical bubbling fluidized bed boilers.



### 3 Results

The calculated phase partitioning of Co, Cu and Sb from the equilibrium calculation using the mean concentration of components of the waste wood, see Table 1, is first presented. Then the results of the sensitivity analysis to Cl and S concentration are presented. Finally a strategy to enrich Sb is presented.

#### 3.1 Base case: Phase partitioning of Co, Cu, and Sb

##### 3.1.1 Cobalt

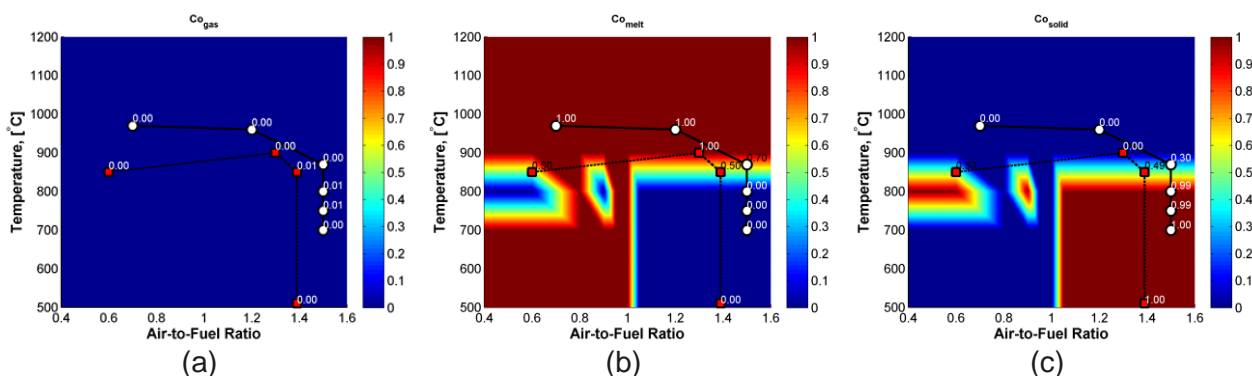


Figure 7. Phase partitioning of cobalt (a) gas (b) melt (c) solid.

Cobalt is non-volatile and remains as part of the solid or molten phase (Figure 7). At the primary to tertiary air zone majority of the Co is in the molten phase. At the post combustion zone where the temperature is below 800°C, cobalt is mostly in the solid phase.

This means that most of the cobalt fed to the boiler may be present as part of the molten ash. This ash has the tendency to stick in the walls of the boiler or cause bed agglomeration if the extent is severe. Cobalt ending up in the fly ash might be present in the coarse particle fraction of the fly ash.

Major species of the cobalt in the molten phase and solid phases are shown in Table 2 and Table 3, respectively.

Table 2. Major species of Co in the molten phase. Table 3. Major species of Co in the solid phase.

T	$\lambda$	Species	T	$\lambda$	Species
< 800°C	< 1	CoS <sub>(SlagA)</sub>	~ 800°C	< 1	Co <sub>(s2)</sub> Metallic Co
> 800 °C	< 1	CoO <sub>(SlagA)</sub>	< 800 °C	>1	(CoO)(TiO <sub>2</sub> ) <sub>(s)</sub>
	>1				



### 3.1.2 Copper

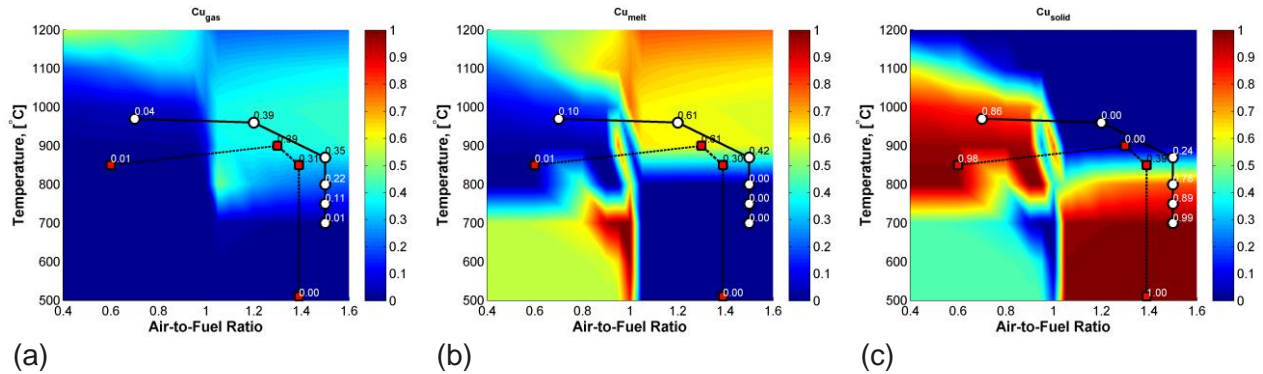


Figure 8. Phase partitioning of copper (a) gas (b) melt (c) solid.

Copper can be found in all phases depending on the temperature and  $\lambda$ . At the splash zone, majority of Cu is in the solid phase. At the secondary and tertiary air zone, Cu is present as part of the melt (ca. 60%) and gaseous phase (ca. 40%). At the post combustion zone where the temperature is less than 800°C, copper exists mostly as solid.

Cu may end up in the bottom ash because it is mostly solid in the splash zone. Cu ending up in the fly ash might be present in the finer fraction of the fly ash, this because of the gas-to-solid phase change during the cooling of the flue gas.

Major species of the copper in the gas, molten, and solid phases are listed in the Table 4, Table 5 and Table 6.

Table 4. Major species of Cu in the gas phase.

T	$\lambda$	Species
> 1000°C	< 1	$\text{Cu}_{(g)}$
> 800 °C	> 1	$\text{CuCl}_{(g)}$ $(\text{CuCl})_{3(g)}$

Table 5. Major species of Cu in the molten phase.

T	$\lambda$	Species
< 800 °C - ~ 900 °C	<~ 1	$\text{Cu}_2\text{S}_{(slag)}$
> 800°C	< 1	$\text{Cu}_2\text{O}_{(slag)}$
> 800°C	> 1	

Table 6. Major species of Cu in the solid phase.

T	$\lambda$	Species
< 800 °C	< 1	$\text{Cu}_3\text{As}_{(s)}$
> 800°C	< 1	$\text{Cu}_{(s)}$ and $\text{Cu}_2\text{S}_{(s3)}$
< 800°C	> 1	$(\text{CuO})(\text{Fe}_2\text{O}_3)_{(s3,s2)}$



### 3.1.3 Antimony

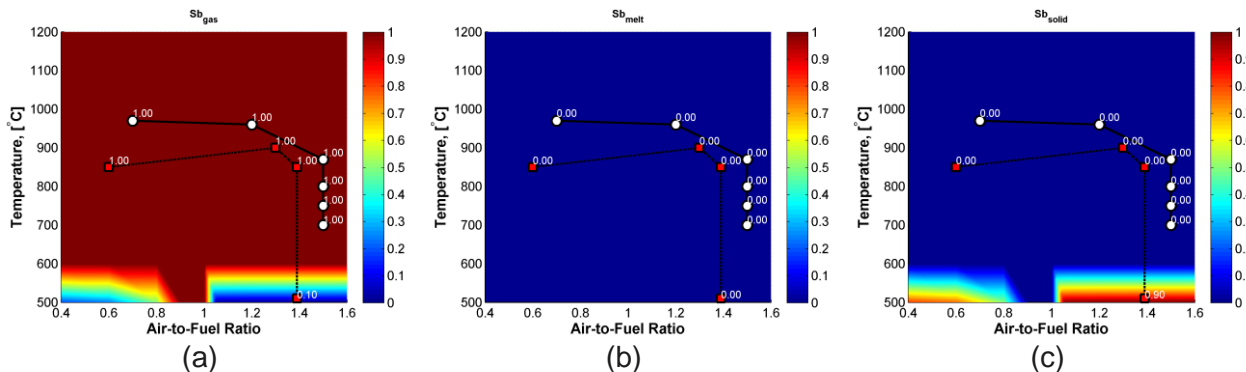


Figure 9. Phase partitioning of antimony (a) gas (b) melt (c) solid.

Antimony can be found mostly in the gas phase, however when the gas is cooled to  $T < 600^{\circ}\text{C}$  (at  $\lambda > 1$ ) Sb condenses, see Figure 9. No antimony is found in the molten phase.

From the splash to the tertiary air zone and superheater area of the boiler, Sb is mostly in the gas phase. After the superheater, antimony condenses to the solid phase. Sb exits the boiler as part of the flue gas (if not captured in ESP or scrubbers) or the fly ash. Sb ending up in the fly ash might be present in the finer fraction of the fly ash, because of the gas-to-solid phase change during the cooling of the flue gas.

Major species of the antimony in the gas and solid phases are listed in Table 7 and Table 8, respectively.

Table 7. Major species of Sb in the gas phase.

T	$\lambda$	Species
Any with gaseous species	Any with gaseous species	$\text{SbO}_{(g)}$

Table 8. Major species of Sb in the solid phase.

T	$\lambda$	Species
$< 600^{\circ}\text{C}$	$< 1$	$\text{NiSb}_{(s)}$
$< 600^{\circ}\text{C}$	$> 1$	$\text{Sb}_2\text{O}_{5(s)}$



### 3.2 Sensitivity Analysis: Effect of varying Cl concentration

Chlorine concentration was varied according to the range of Cl concentration measured from various waste wood fuel ultimate analysis. The objective is to see how the phase partitioning of Co, Cu and Sb will vary as the concentration of Cl is increased from the lowest level to the highest level. The levels analysed are shown in Table 9.

Table 9. Levels of Cl concentration analysed.

Levels	Concentration [wt-% (d.s.) ]
High	0.36
Base	0.17
Low	0.05

#### 3.2.1 Cobalt

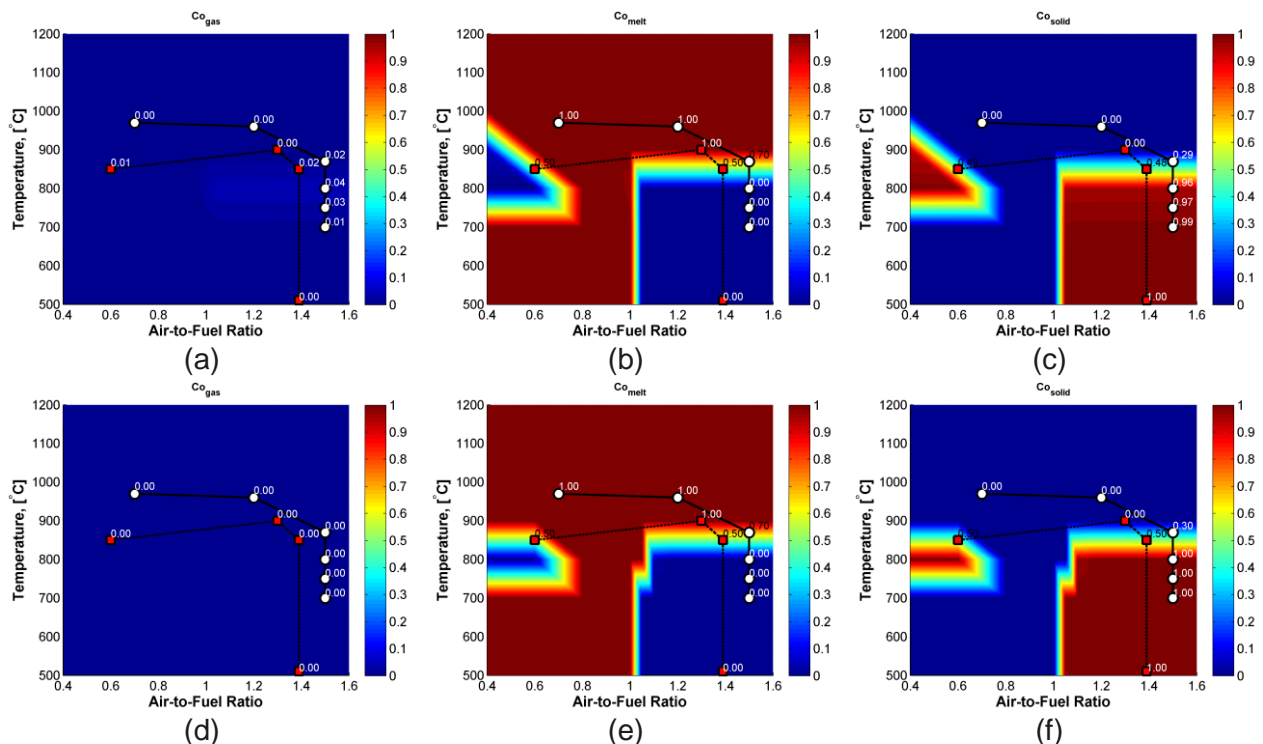


Figure 10. Phase partitioning of cobalt in (a) gas (b) melt (c) solid phases at high Cl level and (d) gas (e) melt (f) solid phases at low Cl level.

Variation in Cl concentration, see Figure 10, has no significant effect on the gas phase partitioning of Co, but there is formation of some  $\text{CoCl}_2(g)$  species ( $<5\%$  of  $\text{Co}_{\text{input}}$ ) at high Cl concentration ( $\sim 800^\circ\text{C}$ ,  $\lambda > 1$ ). In addition, variation in Cl concentration does not significantly change the phase partitioning of Co in between the molten and the solid phase. Along the boiler profiles, the change in Cl concentration does not significantly affect the phase partitioning of Co between molten and solid phase. Co can be found in the melt from the splash zone until the tertiary air zone. As the flue gas cools, near and after superheaters Co is mostly solid, majority as  $(\text{CoO})(\text{TiO}_2)_{(s)}$ .



### 3.2.2 Copper

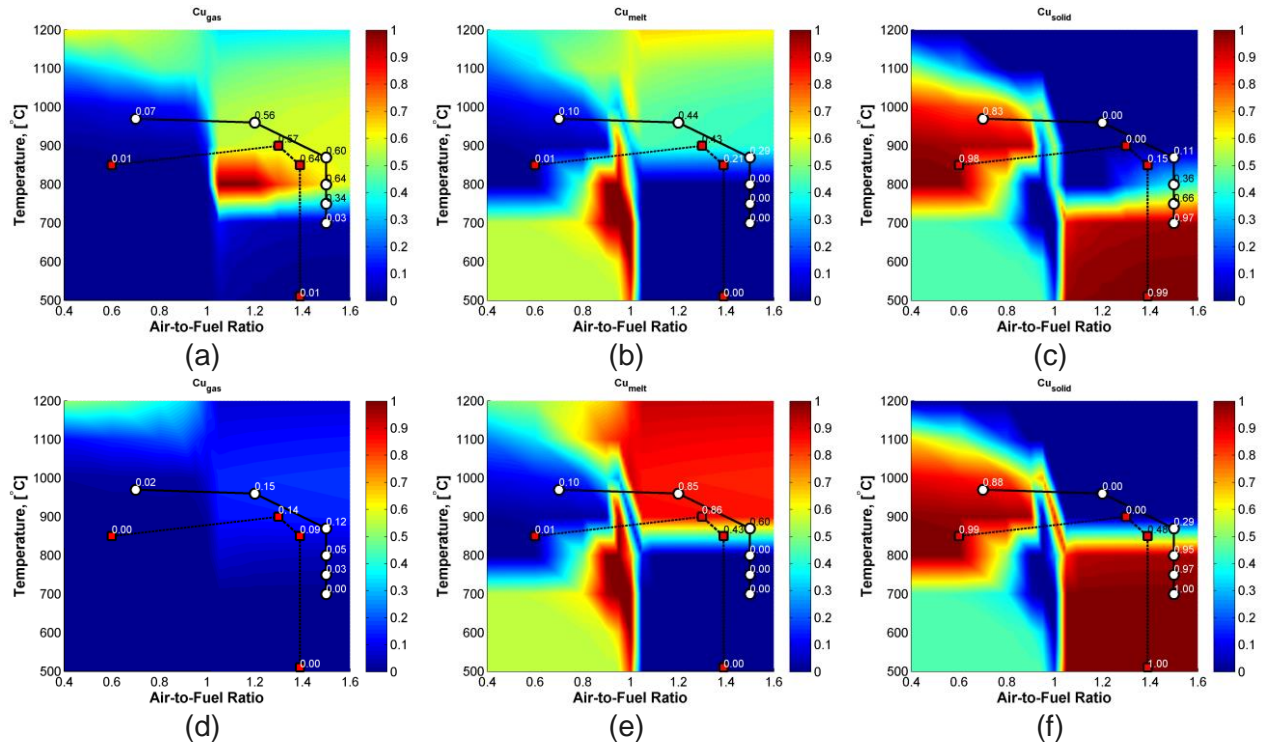


Figure 11. Phase partitioning of copper in (a) gas (b) melt (c) solid phases at high Cl level and (d) gas (e) melt (f) solid phases at low Cl level.

Increasing Cl concentration (low to high level) increases the partitioning of Cu in the gas phase due to the enhanced formation of  $\text{CuCl}_{(g)}$  and  $(\text{CuCl})_{3(g)}$ , (Figure 11). The inverse happens for the partitioning of Cu to molten phase at reducing condition - formation of  $\text{Cu}_2\text{O}_{(FTOXid)}$  is reduced. The partitioning of Cu to the solid phase slightly decreases too, the amount of  $\text{Cu}_{(s)}$  and  $(\text{CuO})(\text{Fe}_2\text{O}_3)_{(s3,s2)}$  formed are reduced.

In the splash zone, majority of the Cu is found in the solid phase regardless of the Cl concentration. At the secondary and tertiary air zones, increasing Cl concentration favours the formation of more gaseous Cu species e.g.  $\text{CuCl}_{(g)}$  and  $(\text{CuCl})_{3(g)}$  at the expense of molten and solid Cu species.

As the flue gas cools around the superheater area, increasing Cl concentration tends to decrease the amount of condensed Cu species and promotes the formation of gaseous Cu species.

After the superheaters, most of the Cu exit the boiler in the solid phase as  $(\text{CuO})(\text{Fe}_2\text{O}_3)_{(s3,s2)}$  regardless of the change in Cl concentration.



### 3.2.3 Antimony

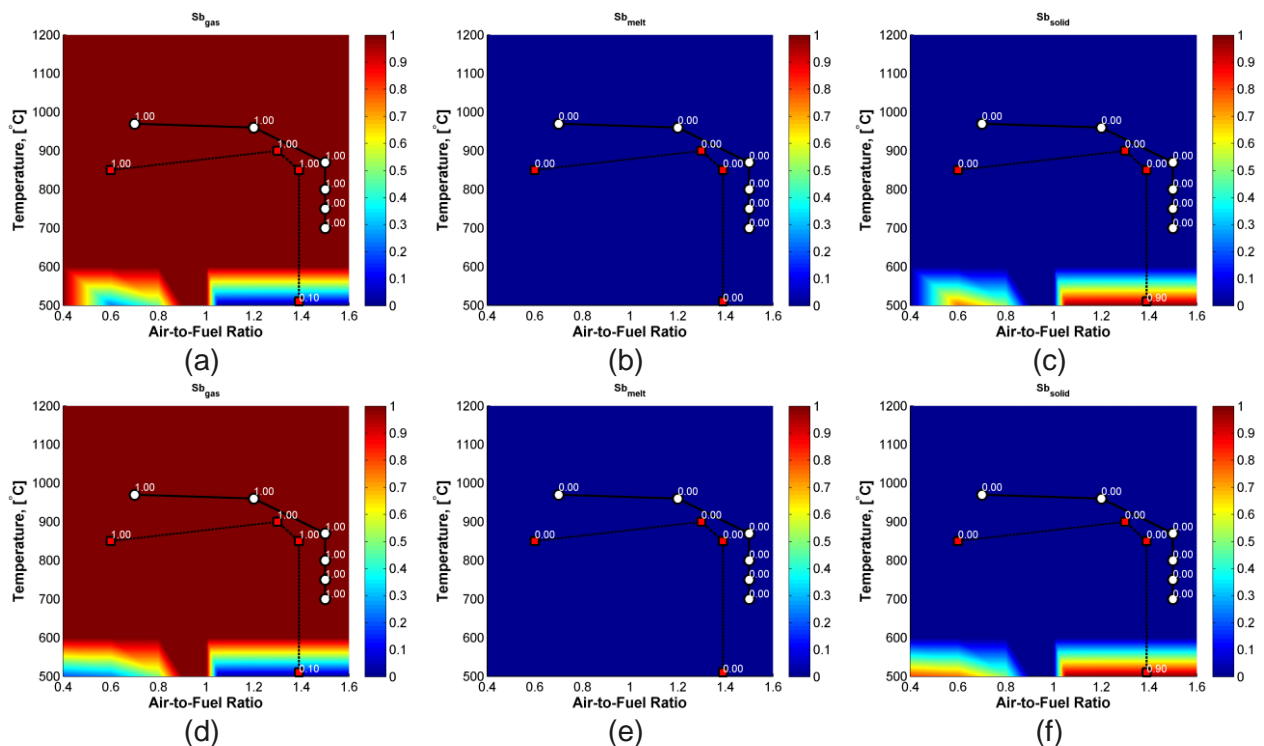


Figure 12. Phase partitioning of antimony in (a) gas (b) melt (c) solid phases at high Cl level and (d) gas (e) melt (f) solid phases at low Cl level.

Increasing Cl concentration (low to high level) does not significantly affect the phase partitioning of antimony. From the splash zone to the superheater region, Sb is found in the gas phase as  $\text{SbO}_{(g)}$ , Figure 12. After the superheaters, ~90% of Sb in the feed condenses and forms  $\text{Sb}_2\text{O}_{5(s)}$ , the rest remains in the gas phase as  $\text{SbO}_{(g)}$ .

### 3.2.4 Summary of importance of varying Cl concentration

In general increasing the chlorine concentration at the levels studied does not significantly affect the phase partitioning of Co and Sb. However, gas phase partitioning of Cu is enhanced as the concentration of Cl is increased.



### 3.3 Sensitivity Analysis: Effect of varying S concentration

Sulphur concentration was varied according to the range of S concentration measured from various waste wood fuel ultimate analysis. The objective is to see how the phase partitioning of Co, Cu and Sb will vary as the concentration of S is increased from the lowest level to the highest level. The levels analysed are shown in Table 10.

Table 10. Levels of S concentration analysed.

Levels	Concentration [wt-% (d.s.) ]
High	0.09
Base	0.07
Low	0.04

#### 3.3.1 Cobalt

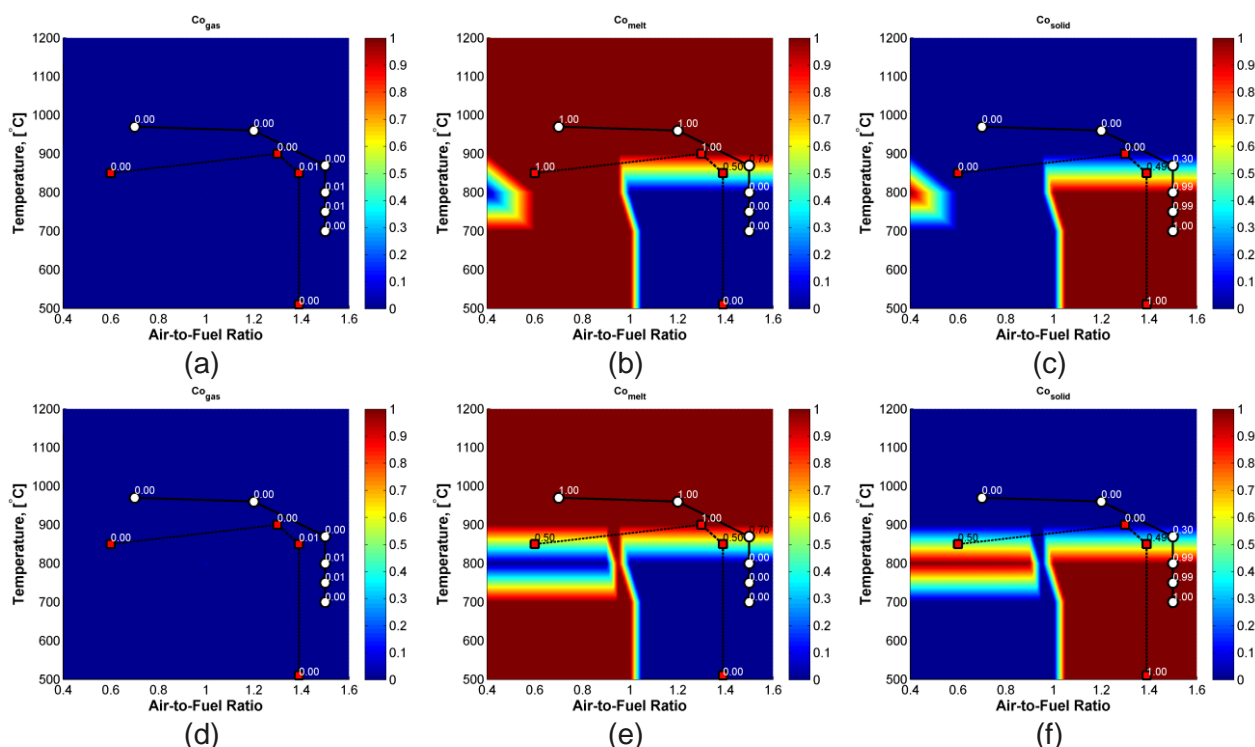


Figure 13. Phase partitioning of cobalt in (a) gas (b) melt (c) solid phases at high S level and (d) gas (e) melt (f) solid phases at low S level.

Variation in S concentration has no significant effect on the gas phase partitioning of Co; that is for all cases considered  $\phi_{Co,gas} \sim 0$ , see Figure 13. Similarly, increasing the concentration of S does not significantly change the phase partitioning of Co to the solid and molten phases. Only certain regions in the T- $\lambda$  surface showed change. For example at 700°C – 900°C and  $0.8 < \lambda < 1$ , the formation of  $CoO_{(FTOXid)}$ , and  $CoS_{(FTOXid)}$  increases the  $\phi_{Co,melt}$ .



Along the boiler profile, increasing S increases the amount of Co ending up in the melt (for Boiler 2). The phase partitioning in all zones from and after the secondary air zone is not affected by the variation in S concentration. For all levels of S tested, Co leaves the boiler as  $(\text{CoO})(\text{TiO}_2)_{(s)}$ .

### 3.3.2 Copper

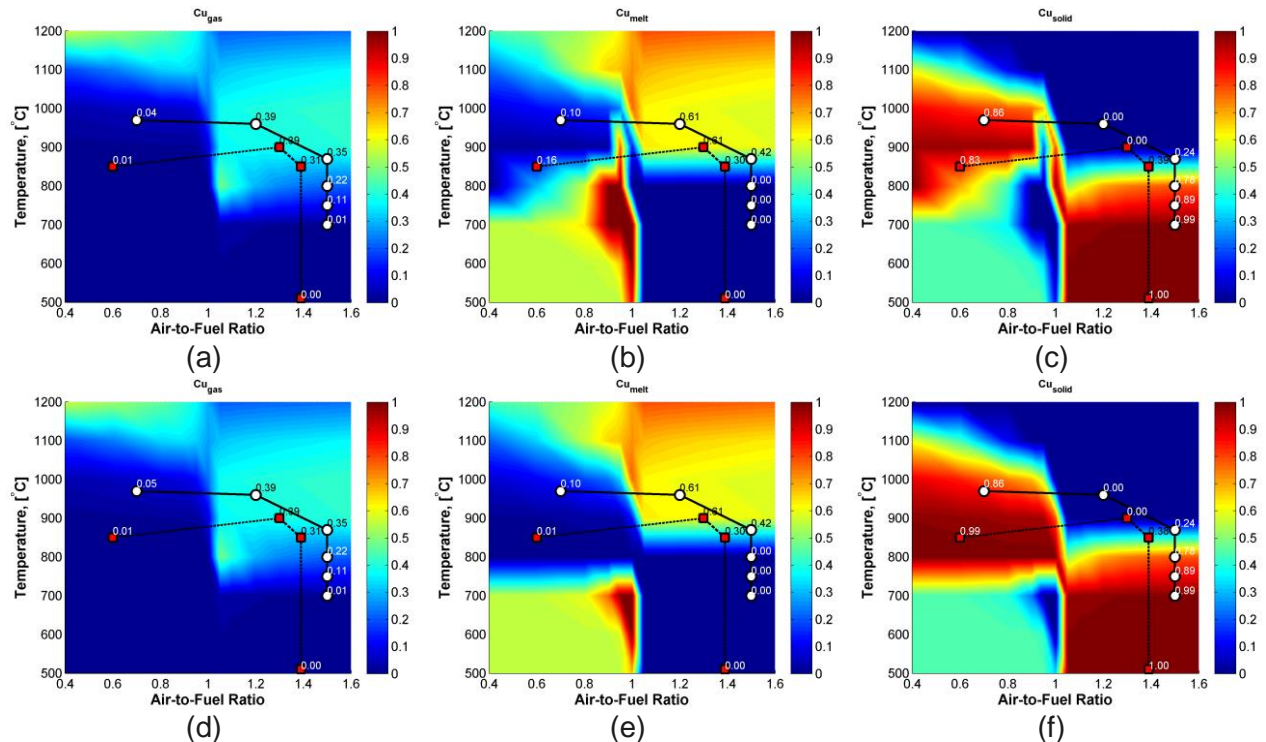


Figure 14. Phase partitioning of copper in (a) gas (b) melt (c) solid phases at high Cl level and (d) gas (e) melt (f) solid phases at low S level.

Increasing S concentration (low to high level) does not affect the gas phase partitioning of Cu; but it promotes the molten phase partitioning of Cu due to the enhanced formation of  $\text{Cu}_2\text{S}_{(\text{FTOxid})}$  at  $800^\circ\text{C} - 900^\circ\text{C}$  and  $\lambda < 1$ , Figure 14. In the same T- $\lambda$  region the solid phase partitioning of Cu decreases due to the loss of  $\text{Cu}_{(s)}$ .

Along the boiler profile, increasing S increases the amount of Cu in the molten phase (for boiler 2). The phase partitioning in all zones from and after the secondary air zone is not affected by the variation in S concentration. For all levels of S tested, Cu leaves the boiler as  $(\text{CuO})(\text{Fe}_2\text{O}_3)_{(s2)}$ .



### 3.3.3 Antimony

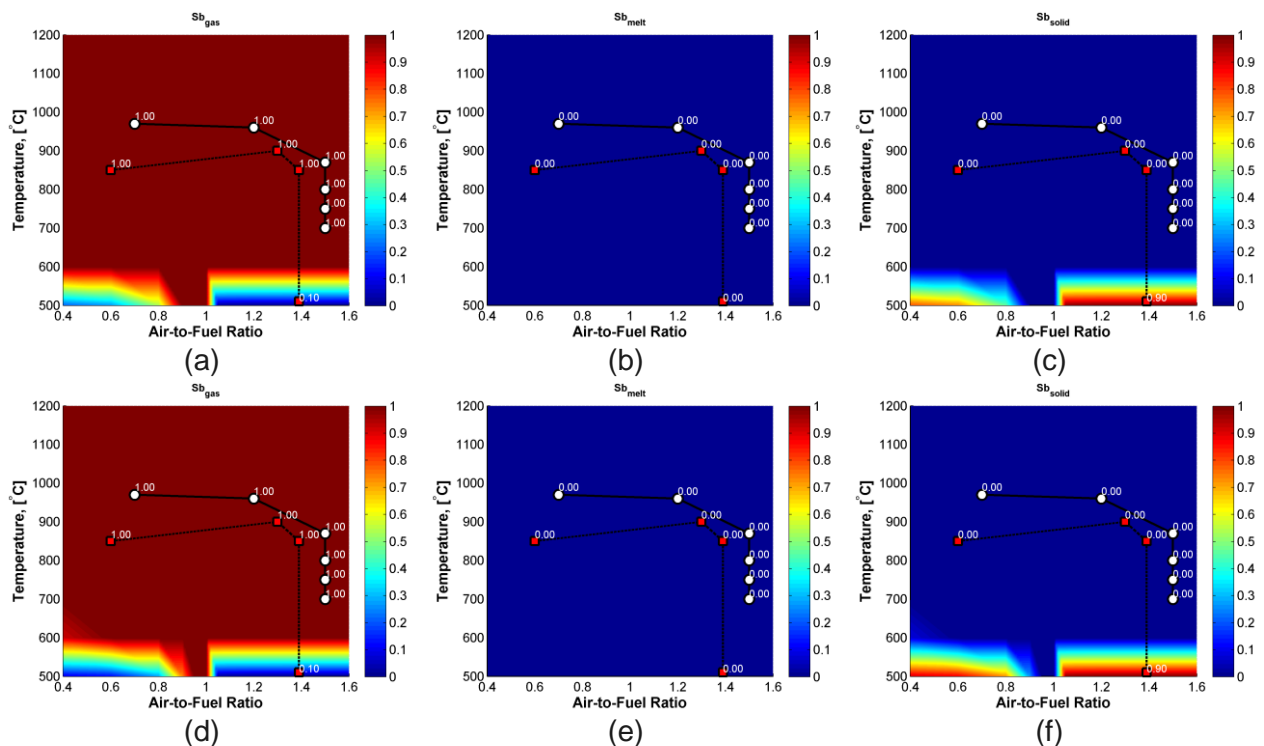


Figure 15. Phase partitioning of antimony in (a) gas (b) melt (c) solid phases at high S level and (d) gas (e) melt (f) solid phases at low S level.

Increasing S concentration (low to high level) does not significantly affect the phase partitioning of antimony, Figure 15. From the splash zone to the superheater region, Sb is found in the gas phase as  $\text{SbO}_{(g)}$ . After the superheaters, ~90% Sb in the feed condenses and forms  $\text{Sb}_2\text{O}_{5(s)}$  the rest remains in the gas phase as  $\text{SbO}_{(g)}$ .

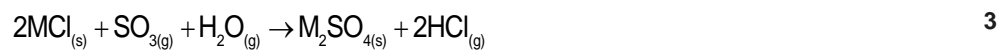
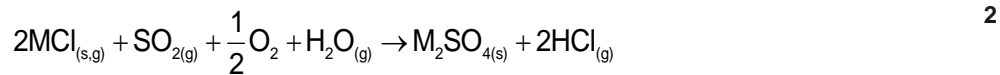
### 3.3.4 Summary of importance of varying S concentration

In general increasing the sulphur concentration at the levels studied does not significantly affect the phase partitioning of Co and Sb. However, the molten phase partitioning of Cu is enhanced as the concentration of S is increased.



## 4 Effect of Additive

Sulphur based additive are often used to combat Cl – induced corrosion of superheater surfaces in boilers fired with challenging fuels such as SRF [11–13]. Sulphur converts risky alkali chlorides, which condense in the superheater region, to alkali sulphates via the reactions:



where M = Na, K.

The phase partitioning of Co, Cu and Sb during the addition of elemental sulphur is presented in this section. Elemental sulphur is added to the fuel to reach a  $S_{total}/Cl_{fuel} = 3$  mol/mol. This value is slightly below the dosing level studied in [13] which is around 4.2 – 4.5 mol/mol.

The phase partitioning Co during elemental sulphur addition is shown in Figure 16. Relative to Figure 7, the gas phase partitioning of Co is not affected by sulphur dosing. This observation is also true for the molten and solid phase partitioning; except in the region  $700^\circ C > T > 900^\circ C$  and  $\lambda < 1$  where molten phase partitioning is enhanced. Along the boiler profile, the phase partitioning is also constant relative to the base case (see section 3.1.1), except for the splash zone of boiler 2, see encircled region in Figure 16.

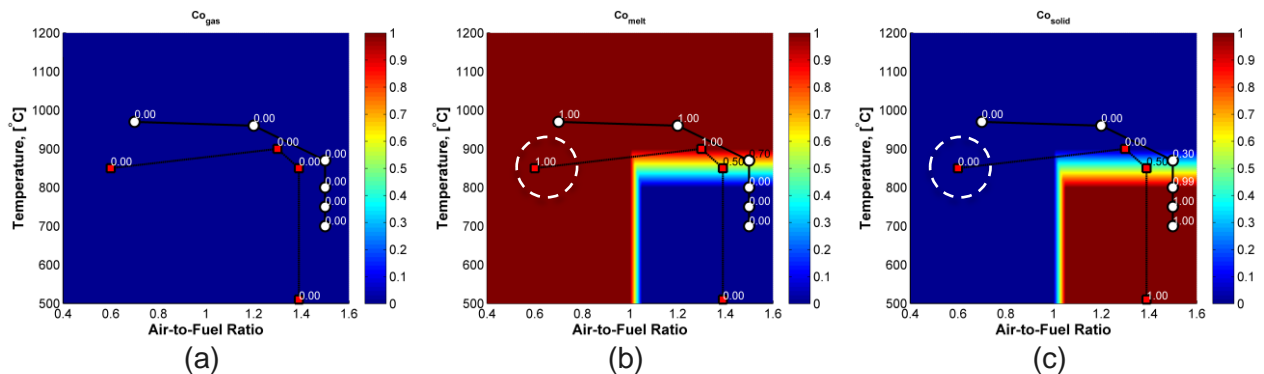


Figure 16. Phase partitioning of Co during elemental sulphur addition.

The phase partitioning of Cu during elemental sulphur addition is shown in Figure 17. Relative to Figure 7, the gas phase partitioning of Cu is not affected by sulphur dosing. Meanwhile the molten phase partitioning in the reducing condition has significantly increased during sulphur dosing. This is due to enhanced formation of  $Cu_2S_{(slag)}$ . The phase partitioning of Cu in the splash zone of both boilers have changed significantly relative to the base case discussed in section 3.1.2. For the other zones of the boiler the phase partitioning has remained the same.

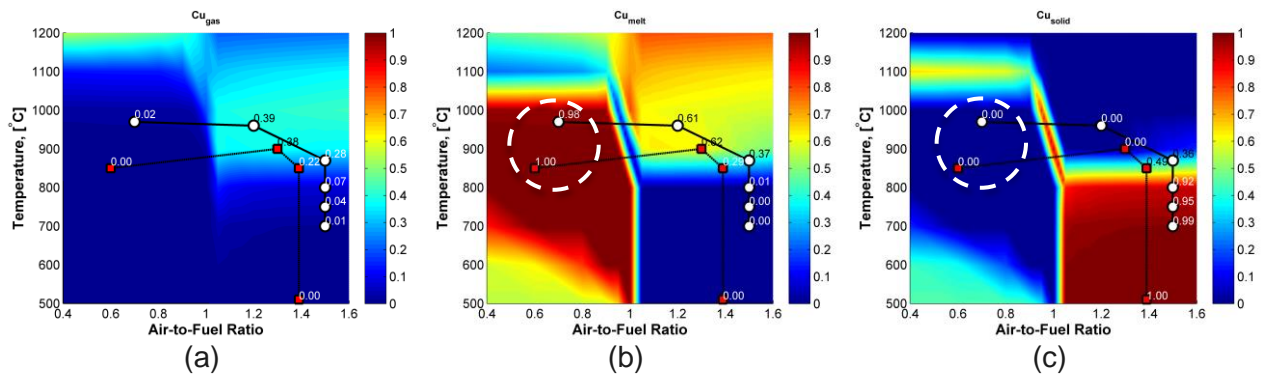


Figure 17. Phase partitioning of Cu during elemental sulphur addition.

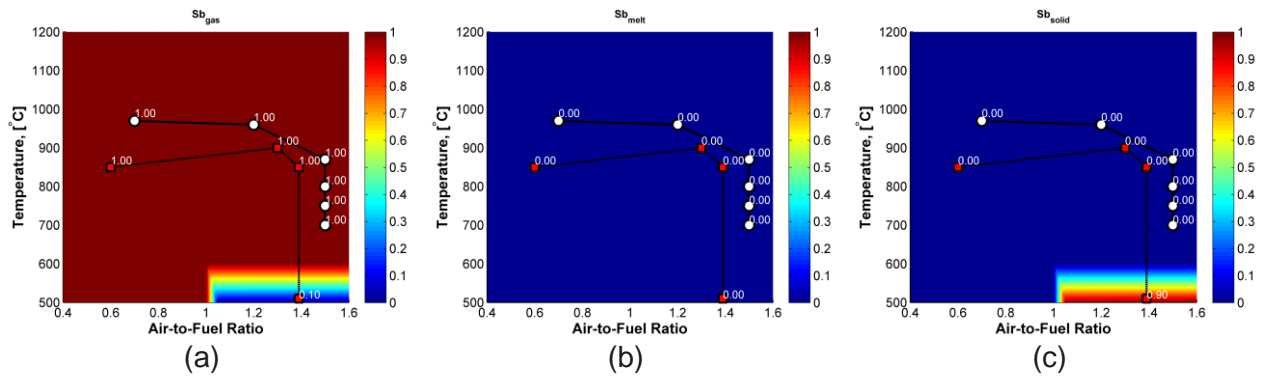


Figure 18. Phase partitioning of Sb during elemental sulphur addition.

The phase partitioning of Sb during elemental sulphur addition is shown in Figure 18. Relative to the base case (see section 3.1.3), no change in phase partitioning of Sb is detected by the model during elemental sulphur addition. The phase partitioning along the boiler profile also did not change.

## 5 Discussion

Among the elements analysed, antimony has the most potential of in-situ enrichment in the boiler (to the desired fly ash fraction) because of the narrow temperature range required for the gas-to-solid phase transition. The figure below shows this range.

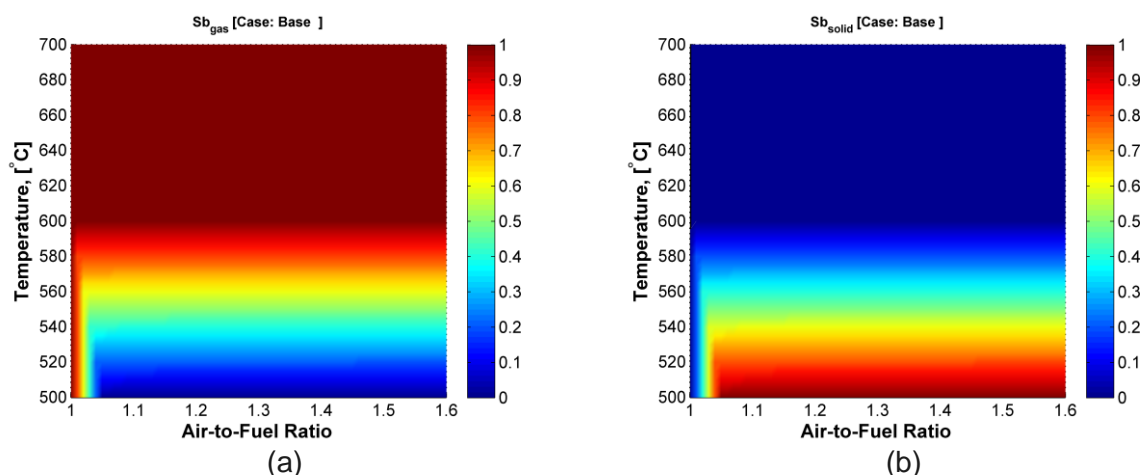


Figure 19. Gas and solid phase partitioning calculated for Sb. This figure is a zoomed-in section of Figure 9.

One possible strategy to enrich antimony for example to scrubber precipitate is to collect major fly ash stream at around 600°C with the use of a hot cyclone. At 600°C < T < 700°C, where major ash forming elements<sup>1</sup> and trace elements<sup>2</sup> are almost entirely in the solid phase ( $0.9 < \phi_{i,gas} \leq 1.0$ ). At same temperature range, around 80-90% of K, N, S, and Zn have also condensed. The remained fraction of these elements and almost all Sb can pass the hot cyclone in the flue gas and can be collected later in the gas scrubber as part of the precipitate.

The hot cyclone discussed already above can have two functions (a) to circulate sand to the furnace (return cyclone for circulating fluidized bed mode) and (b) to separate fly ashes. The flue gas is then sent to a scrubber where Sb is collected as part of the precipitate. The operating principle is illustrated in Figure 20.

<sup>1</sup> Al, Ba, Ca, Fe, Mg, Mn, P, Si, Ti

<sup>2</sup> As, Co, Cu, Ni, V

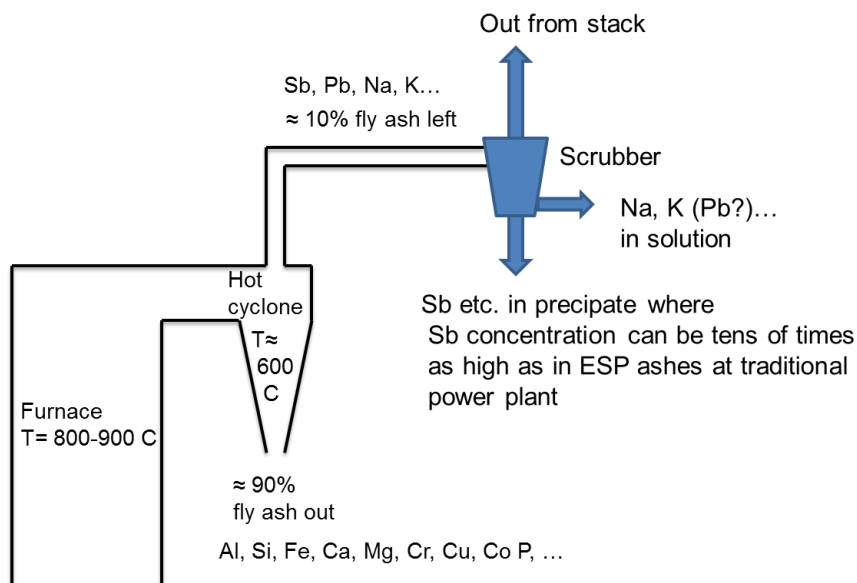


Figure 20. Operating principle of Sb enrichment process.

To validate the modelling results presented, VTT's fluidized bed boilers can be employed. For example in the BFB, see Figure 21, the cyclone temperature can be varied to test how temperature affects the concentration of Sb in the cyclone ash. The temperature levels of the cyclone can be selected on the basis of the modelling results of the gas to solid phase transition shown in Figure 19.

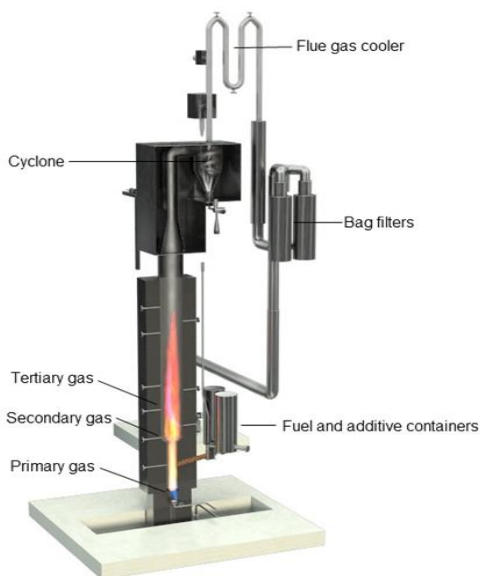


Figure 21. VTT's 20 kW bubbling fluidized bed pilot facility.

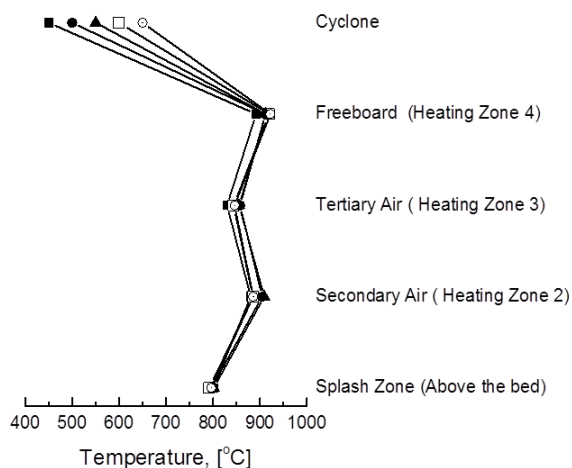


Figure 22. Temperature profile of the BFB pilot reaction showing possible temperature settings for the cyclone.

Using the same device, the concentration of other metals in the fine particle fraction of the fly ash can also be monitored.



## 6 Conclusion and recommendation

Thermodynamic equilibrium calculations revealed the behaviour of Co, Cu, and Sb during the combustion of waste wood. In the BFB boiler, Co can be found mostly in the melt and may leave the boiler as part of the coarse fraction of the fly ash. Cu may end up as part of the bottom ash, or part of the fine fraction of the fly ash. Sb is mostly gas inside the BFB boiler, and may leave the boiler mostly as part of the fine particle fraction of the fly ash.

Among the elements tested, only Sb exhibits a very narrow temperature range of gas-to-solid phase transition. This unique behaviour of Sb can be used to concentrate the element to the desired fly ash stream.

Because thermodynamic equilibrium calculation has its limitations, it is recommended to perform pilot scale combustion experiments to validate the results obtained from the calculations.



## 7 References

- [1] Clarke, L. B., and Sloss, L. L., 1992, Trace elements - emissions from coal combustion and gasification, IEA Coal Research.
- [2] Lundholm, K., Nordin, A., and Backman, R., 2007, Trace element speciation in combustion processes—Review and compilations of thermodynamic data, *Fuel Process. Technol.*, **88**(11-12), pp. 1061–1070.
- [3] Hupa, M., 2012, Thermodynamic Modeling of Combustion Processes – Applications and Limitations, Chemical Thermodynamics in Furnaces a joint symposium and course for combustion specialists and metallurgists.
- [4] Lindberg, D., Backman, R., Chartrand, P., and Hupa, M., 2011, Towards a comprehensive thermodynamic database for ash-forming elements in biomass and waste combustion — Current situation and future developments, *Fuel Process. Technol.*, **105**, pp. 129–141.
- [5] Konttinen, J., Backman, R., Hupa, M., Moilanen, A., and Kurkela, E., 2013, Trace element behavior in the fluidized bed gasification of solid recovered fuels – A thermodynamic study, *Fuel*, **106**, pp. 621–631.
- [6] Koukkari, P., Penttillä, K., and Karema, H., 2009, New Dynamics for kiln chemistry, *Advance Gibbs Energy Methods for Functional Materials and Processes ChemSheet 1999-2009*, P. Koukkari, ed., Helsinki, pp. 117–123.
- [7] Talonen, T., 2008, Chemical Equilibria of Heavy Metals in Waste Incineration: Comparison of Thermodynamic Databases, Åbo University.
- [8] Sandelin, K., and Backman, R., 1999, A Simple Two-Reactor Method for Predicting Distribution of Trace Elements in Combustion Systems, *Environ. Sci. Technol.*, **33**(24), pp. 4508–4513.
- [9] Bankiewicz, D., Vainikka, P., Lindberg, D., Frantsi, A., Silvennoinen, J., Yrjas, P., and Hupa, M., 2012, High temperature corrosion of boiler waterwalls induced by chlorides and bromides – Part 2: Lab-scale corrosion tests and thermodynamic equilibrium modeling of ash and gaseous species, *Fuel*, **94**, pp. 240–250.
- [10] Becidan, M., Sørnum, L., Frandsen, F., and Pedersen, A. J., 2009, Corrosion in waste-fired boilers: A thermodynamic study, *Fuel*, **88**(4), pp. 595–604.
- [11] Aho, M., Vainikka, P., Taipale, R., and Yrjas, P., 2008, Effective new chemicals to prevent corrosion due to chlorine in power plant superheaters, *Fuel*, **87**(6), pp. 647–654.
- [12] Kassman, H., Bäfver, L., and Åmand, L.-E., 2010, The importance of SO<sub>2</sub> and SO<sub>3</sub> for sulphation of gaseous KCl – An experimental investigation in a biomass fired CFB boiler, *Combust. Flame*, **157**(9), pp. 1649–1657.
- [13] Bajamundi, C. J. E., Vainikka, P., Hedman, M., Silvennoinen, J., Heinanen, T., Taipale, R., and Konttinen, J., 2015, Searching for a robust strategy for minimizing alkali chlorides in fluidized bed boilers during burning of high SRF-energy-share fuel, *Fuel*, **155**, pp. 25–36.